# Pressure-induced Kondo semiconductor: The filled skutterudite compound $CeRu_4Sb_{12}$

N. Kurita,[1,2,*] M. Hedo,[3] M. Koeda,[1] M. Kobayashi,[4] H. Sato,[4] H. Sugawara,[5] and Y. Uwatoko[1]

[1]*Institute for Solid State Physics, University of Tokyo, Chiba 277-8581, Japan*
[2]*Los Alamos National Laboratory, Los Alamos, New Mexico 87545, USA*
[3]*Faculty of Science, University of the Ryukyus, Nishihara, Okinawa 903-0213, Japan*
[4]*Department of Physics, Tokyo Metropolitan University, Tokyo 192-0397, Japan*
[5]*Faculty of Integrated Arts and Science, The University of Tokushima, Tokushima 770-8502, Japan*

We report electrical transport and x-ray studies under high pressure of the filled skutterudite compound $CeRu_4Sb_{12}$. Electrical resistivity measurements in the temperature range 2–300 K and under hydrostatic pressures up to 10.0 GPa have revealed a pressure-induced metal-semiconductor transition above 5.0 GPa in $CeRu_4Sb_{12}$. The energy gap in the semiconducting state of $CeRu_4Sb_{12}$ estimated from an activation law increases with a pressure coefficient of $\sim$12 K/GPa. On the other hand, a high-pressure x-ray study has determined the relationship between lattice constant and energy gap of $CeRu_4Sb_{12}$ under high pressure. We suggest that an electronic mechanism of a semiconducting state in $CeRu_4Sb_{12}$ under high pressure could originate from an enhanced $c-f$ hybridization and that the $P$-induced state could be categorized as a Kondo semiconductor.

## I. INTRODUCTION

Filled skutterudite compounds $RT_4X_{12}$ ($R$=rare earth; $T$=Fe, Ru, Os; $X$=P, As, Sb) crystallize in the body-centered cubic structure with a space group $Im\bar{3}$. The $RT_4X_{12}$ family has attracted much attention since they exhibit a wide variety of ground states at low temperature (LT), such as superconductivity in $LaT_4X_{12}$,[1–6] heavy fermion superconductivity in $PrOs_4Sb_{12}$,[7] scalar ordering in $PrFe_4P_{12}$,[8–10] heavy fermion ferromagnetism in $SmFe_4P_{12}$,[11] and a metal-insulator (MI) transition in $PrRu_4P_{12}$ and $SmRu_4P_{12}$.[12,13] These features can be explained by strong $c-f$ hybridization, a unique band structure and an orbital degree of freedom originated from the $4f$ electrons in the $R$ site with their unique cubic symmetry.[14] Among them, Ce-based $CeT_4X_{12}$ compounds have quite different characteristics. Most of the $CeT_4X_{12}$ compounds show semiconducting behavior with a band gap of 10–1500 K.[15–18] It has been proposed that these semiconducting states can be classified as Kondo semiconductor or Kondo insulator, where $c-f$ hybridization plays an important role, which is strongly supported by the fact that the magnitude of energy gap in $CeT_4X_{12}$ increases with decreasing lattice constant and also by the experimental results with La substitution.[19,20]

Meanwhile, $CeRu_4Sb_{12}$ exhibits metallic behavior at LT, although a result of the band calculation predicts it as an insulator with a small band gap.[21,22] It should be noted that optical conductivity and neutron-scattering measurements confirmed both a charge gap and a spin gap feature, respectively, at LT.[23,24] In this regard, Saso[25] recently succeeded in reproducing the experimental optical conductivity data and the metallic behavior of resistivity in $CeRu_4Sb_{12}$ by using a simplified tight-binding model. Shubnikov-de Haas (SdH) and de Haas-van Alphen (dHvA) experiments clarified the existence of a small Fermi surface at LT with an enhanced effective mass $m^*$.[26–28] It is also noteworthy that $CeRu_4Sb_{12}$ shows novel non-Fermi-liquid (NFL) behavior.[21,29] Applying

pressure at zero field suppresses the NFL state and extends the Fermi liquid (FL) region to the lowest temperature of 0.5 K at 1.3 GPa, which is analogous to the recovery of a FL state under magnetic fields at ambient pressure.[30,31] These unique features in $CeRu_4Sb_{12}$ may be caused by a delicate electronic band structure in the vicinity of the Fermi level.

$CeT_4P_{12}$ compounds have smaller lattice constants than that expected from a trivalent lanthanide contraction.[32,33] It indicates that the Ce ion in $CeT_4P_{12}$ might be intermediate valent, leading to a strong $c-f$ hybridization. On the other hand, since antimonide compounds have a larger lattice constant compared with phosphoride ones, it can be considered that $CeT_4Sb_{12}$ has a weaker $c-f$ hybridization. The tuning strength of the hybridization by applying pressure is, therefore, key to understanding the complicated characteristics in $CeRu_4Sb_{12}$. In fact, our previous pressure experiment up to 8.0 GPa revealed a metal-semiconductor transition in $CeRu_4Sb_{12}$ above 5.0 GPa.[34] In this paper, we report the results of electrical transport and x-ray diffraction measurements of $CeRu_4Sb_{12}$ at high pressures up to 10.0 and $\sim$14 GPa, respectively.

## II. EXPERIMENTAL DETAILS

Single crystals of $CeRu_4Sb_{12}$ were grown by the Sb-self-flux method. High quality of the samples employed in this study is inferred from the clear observation of SdH and dHvA oscillations.[26–28] Electrical resistivity under applied high pressures and fields up to 10.0 GPa and 3.0 T, respectively, were measured for $J\|[100]$ from 2 to 300 K by the standard dc four-probe method. Hydrostatic pressure was generated by using a cubic anvil pressure device with a 250 ton press which is equipped with a superconducting magnet ($0 \le \mu_0H \le 3.5$ T).[35] We used a 1:1 mixture of Fluorinert FC-70 and FC-77 as a pressure-transmitting medium. The specimens employed were of the dimension $\sim$0.8$\times$0.3$\times$0.2 mm$^3$. The electrical contacts with the specimen were

made with 20 $\mu$m diameter gold wires using a conducting silver paste. In electrical resistivity measurements, two different samples were examined: single crystals labeled as 1 and 2 were employed in the measurement at 1.5–8.0 GPa performed by the cubic anvil method with tungsten-carbide (WC) anvils and at 7.0–10.0 GPa by that with sintered-diamond (SD) anvils, respectively. X-ray diffraction measurement under high pressure of $\sim$14 GPa was carried out at room temperature by using an imaging plate and gas-driven-type diamond anvil cell (DAC). In order to generate hydrostatic pressure in DAC, a 4:1 mixture of methanol and ethanol solution was used as the pressure-transmitting medium. The magnitude of pressure in the sample cavity was estimated at room temperature from comparison of the fluorescence of ruby located near the sample to that of another ruby outside the DAC.

### III. RESULTS

Figure 1 shows the temperature dependence of electrical resistivity $\rho(T)$ of CeRu$_4$Sb$_{12}$ under several pressures, (a) 1.5–5.0 GPa, (b) 5.0–8.0 GPa, and (c) 7.0–10.0 GPa. Both the data set in (a) and (b) for sample 1 and the data in (c) for sample 2 were obtained by using cubic anvil method with WC anvils and with SD anvils, respectively. At 1.5 GPa in Fig. 1(a), $\rho(T)$ exhibits a maximum ($T_{\max}$) around 90 K, below which it decreases steeply due to forming coherent Kondo state. Above $T_{\max}$, the resistivity obeys $-\log T$ due to single-ion Kondo effect as seen in the inset. The overall behavior is qualitatively the same as that at ambient pressure.[21] With increasing pressures up to 5.0 GPa, while $\rho(300$ K$)$ shows a minor increase, the broad peaks in $\rho(T)$ around $T_{\max}$ are gradually enhanced and $\rho(T)$ in the LT region increases. At $P\geq6.0$ GPa, $\rho(T)$ behavior is drastically changed especially at LT region. As indicated by an arrow in Fig. 2(a), at 6.0 GPa, $\rho(T)$ exhibits a minimum ($T_{\min}$) around 15 K and then decreases as $T$ decreases below 7 K. With further pressurization up to 8.0 GPa, as shown in Fig. 1(b), a remarkable upturn toward the lowest temperature below $T_{\min}$ is observed, suggesting that the ground state of CeRu$_4$Sb$_{12}$ might be changed from a metallic one to semiconducting one at $P\geq6.0$ GPa. A hump in $\rho(T)$ around $T_{\max}$, which slightly shifts to lower temperature with pressurization, has been still observed at 8.0 GPa. On the other hand, $T_{\min}$ steeply moves to higher temperature, resulting in a merging of $T_{\max}$ and $T_{\min}$ at 9.0 and 10.0 GPa as shown by arrows in Fig. 1(c), which will be discussed later.

In Ce compounds, applying pressure generally increases the magnetic exchange interaction between the localized 4$f$ spins and the conduction electrons ($J_{cf}$). It is because $J_{cf}$ can be simply described as $J_{cf}=V_{cf}^2/|E_F-E_f|$ and, in Ce compounds, the application of pressure increases $V_{cf}$ and decreases $|E_F-E_f|$, where $V_{cf}$ is the matrix element that admixes $f$-electron and conduction-electron states and $|E_F-E_f|$ is the difference between the Fermi level and the energy level of $f$ electrons. As seen from the solid lines in the inset of Figs. 1(a)–1(c), resistivity follows $-\log T$ above $T_{\min}$ or above the temperature indicated by arrows at $P=9.0$ and 10.0 GPa. Figure 2(b) shows the pressure variation of abso-
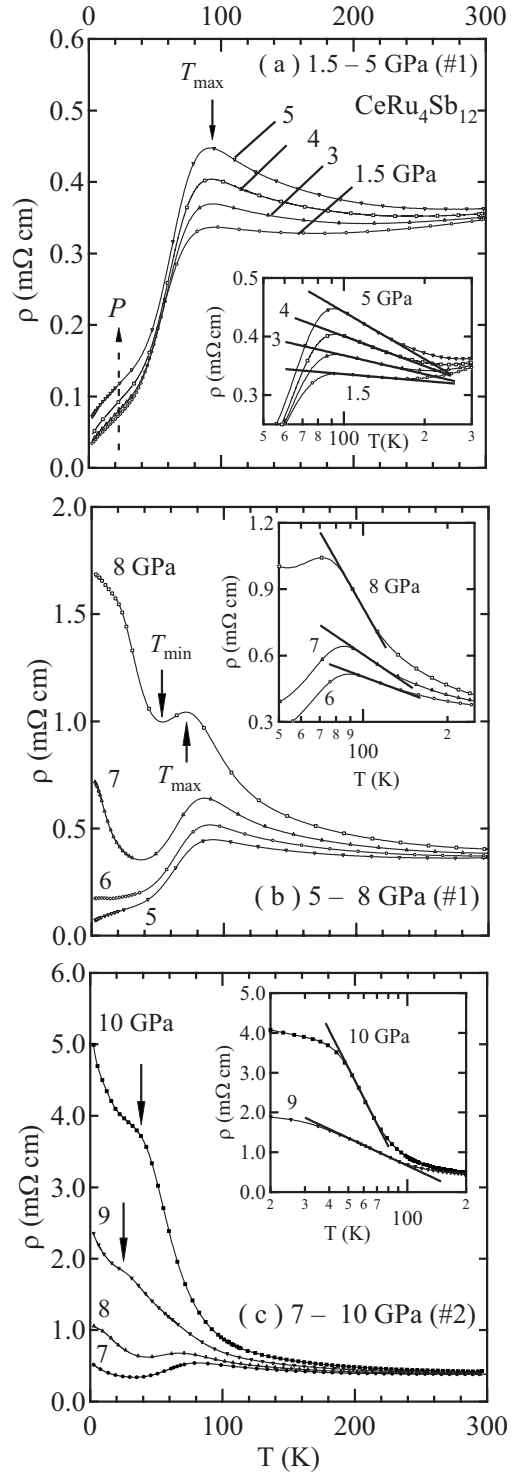


FIG. 1. Temperature dependence of electrical resistivity $\rho(T)$ in CeRu$_4$Sb$_{12}$ at a temperature of 2–300 K under several pressures: (a) 1.5–5.0 GPa, (b) 5.0–8.0 GPa, and (c) 7.0–10.0 GPa. Results in (a) and (b) were obtained by using a cubic anvil pressure device with WC anvils for a sample 1, and the result in (c) was obtained by using one with SD anvils for a sample 2. $T_{\max}$ and $T_{\min}$ are defined as the temperature where $\rho$ shows a maximum and minimum, respectively. Arrows at 9 and 10 GPa in (c) indicate anomalies in $\rho(T)$. The insets in (a), (b), and (c) show $\rho(T)$ as a semilog plot. Solid lines represent the temperature range where resistivity follows $-\log T$ dependence.
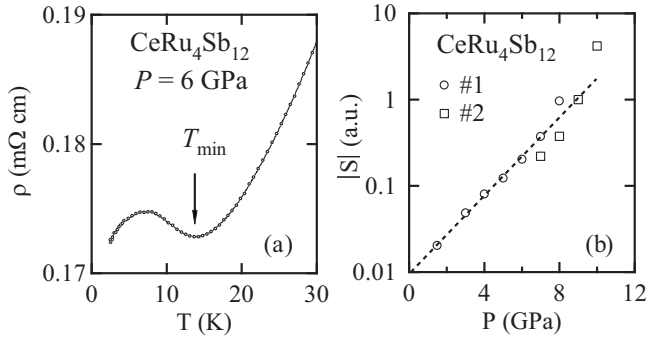
FIG. 2. (a) Low-temperature expansion of $\rho(T)$ at 6.0 GPa in CeRu$_4$Sb$_{12}$. $\rho(T)$ has minimum ($T_{min}$) around 15 K. (b) Pressure variation of the slope $S$ in $\rho \propto -\log T$ of CeRu$_4$Sb$_{12}$. Dashed line is a guide for the eyes.

lute value of slope in the linear $-\log T$ term ($|S|$) in CeRu$_4$Sb$_{12}$. With increasing pressure, $|S|$ increases exponentially. According to the theory of Cornut and Coqblin,[36] $|S|$ is described as a function of $J_{cf}$. At high temperature (HT) above $T_{max}$, the rise of $|S|$ with applying pressure indicates the increase of $J_{cf}$. Therefore, the pressure variation of $|S|$ in CeRu$_4$Sb$_{12}$ is consistent with the enhancement of $J_{cf}$ with pressurization. It should be noted that resistivity data obtained in this study contain a phonon term, which generally reduces the temperature ranges where $\rho \propto -\log T$ and the magnitude of $|S|$. In fact, at ambient pressure, a magnetic term of resistivity $\rho_{mag} = \rho(CeRu_4Sb_{12}) - \rho(LaRu_4Sb_{12})$ exhibits $-\log T$ dependence in a wider temperature range with larger $|S|$.[26] Here, we can see a slight difference in absolute



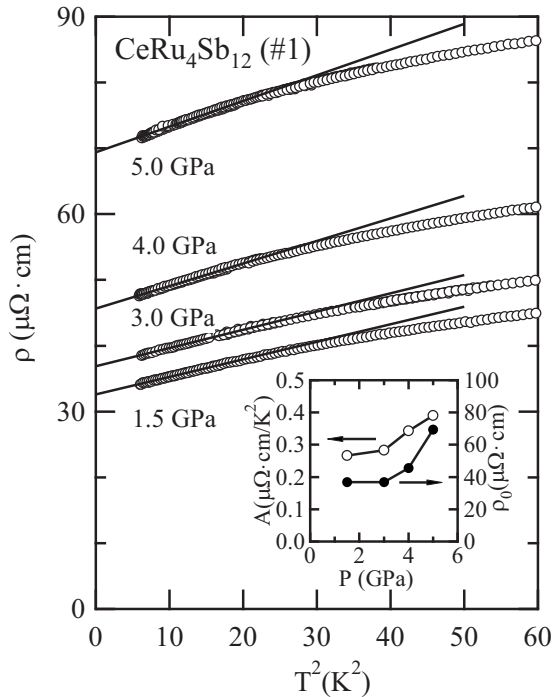FIG. 3. $T^2$ dependence of electrical resistivity of CeRu$_4$Sb$_{12}$ at 1.5–5.0 GPa (sample 1). Straight lines are guides for the eyes indicating the temperature range where $\rho = \rho_0 + AT^2$. Inset shows pressure dependence of $A$ and $\rho_0$ values in CeRu$_4$Sb$_{12}$.
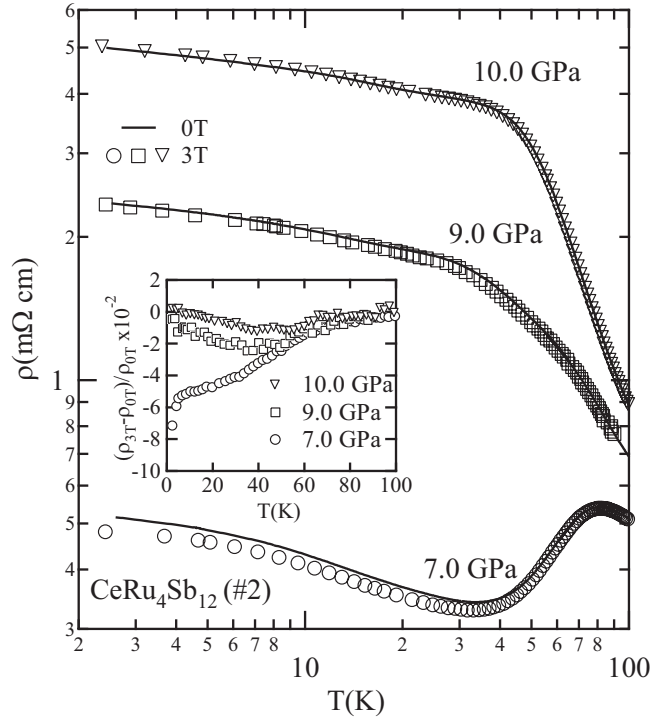


FIG. 4. Pressure effect on $\rho(T)$ of CeRu$_4$Sb$_{12}$ (sample 2) under 0 and 3 T. Solid curves and markers indicate $\rho(T)$ under 0 and 3 T at each pressure, respectively. The inset shows temperature dependence of the terms of magnetic-field effect $(\rho_{3\,T} - \rho_{0\,T})/\rho_{0\,T}$.

value of $\rho(T)$ at 7.0 and 8.0 GPa between Figs. 1(b) and 1(c). It can be explained by the sample dependence and the experimental error in generated pressure between samples 1 and 2, but did not affect the semiconducting behavior itself.

Next, we focus on the result in the LT regime. Kobayashi et al.[31] reported that applying pressure had caused suppression of the NFL behavior at 1.3 GPa, resulting in recovery of FL behavior. In our study, FL behavior, $\rho = \rho_0 + AT^2$, is also observed below 5 K at pressures from 1.5 to 5.0 GPa. At $P \geq 6.0$ GPa, $\rho(T)$ no longer follows FL $T^2$ dependence probably due to a contribution of the $P$-induced semiconductivity. Figure 3 depicts the low-temperature resistivity versus $T^2$ of CeRu$_4$Sb$_{12}$ at pressures up to 5.0 GPa. The straight lines represent the $T^2$ fitting results from a FL law. The inset of Fig. 3 shows the pressure variation of the $A$ value, which corresponds to the slope of the lines and residual resistivity $\rho_0$. With increasing pressure, both $A$ and $\rho_0$ are enhanced especially above 3.0 GPa. $A$ is described as the relation $A \propto \gamma^2 \propto (1/T_K)^2$, where $\gamma$ is Sommerfeld coefficient and $T_K$ is Kondo temperature. In Ce compounds, $T_K$ increases with applying pressure due to the enhancement of $c-f$ hybridization, resulting in decrease in the coefficient $A$. In the case of CeRu$_4$Sb$_{12}$, however, application of pressure has the opposite effect on $A$. This fact suggests that, even below the pressure where $P$-induced semiconducting behavior shows up, resistivity at LT region may be affected not only by electron-electron scattering but also by the scattering related to the semiconductivity.

Figure 4 shows a plot with double-logarithmic scale of $\rho(T)$ at 7.0, 9.0, and 10.0 GPa under magnetic fields of 0 and
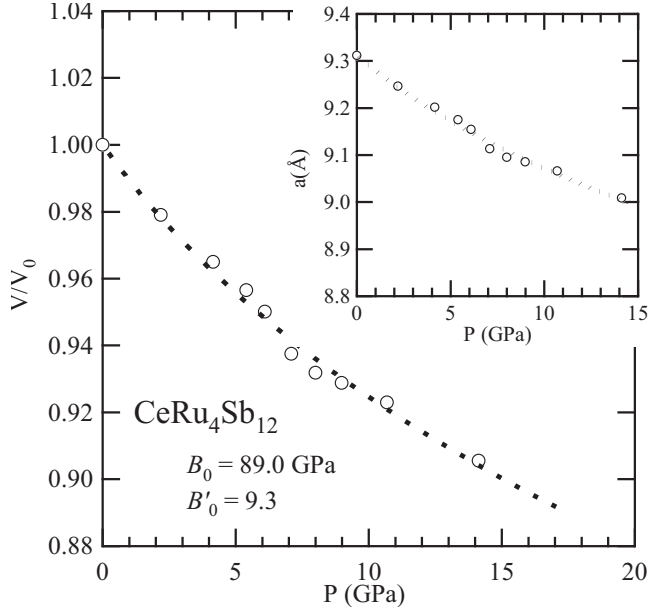
FIG. 5. Relative cell volume ($V/V_0$) versus pressure of $CeRu_4Sb_{12}$. Inset shows pressure dependence of lattice constant of $CeRu_4Sb_{12}$. Dashed lines are fitted based on the Birch-Murnaghan equation of state (1).

3 T in $CeRu_4Sb_{12}$. Straight lines and symbols correspond to the data at 0 and 3 T, respectively. No significant change is observed in $\rho(T)$ up to 3 T at all investigated pressures. A magnetic contribution term, $\Delta\rho(H)/\rho(0)=(\rho_{3\ T}-\rho_{0\ T})/\rho_{0\ T}$, as a function of temperature at each pressure is shown in the inset of Fig. 4. The field of 3 T decreases $\Delta\rho(H)/\rho(0)$ in the investigated temperature range. While $\Delta\rho(H)/\rho(0)$ at 7 GPa monotonically decreases with decreasing temperature, $\Delta\rho(H)/\rho(0)$ at 9.0 and 10.0 GPa shows a broad minimum around 40 K where the anomalous behavior is observed as mentioned in Fig. 1(c). This suggests that the electronic structure below 40 K may be changed above 7.0 GPa. Recently, the ground state of the heavy fermion skutterudite compound $PrFe_4P_{12}$ was found to change from metallic to insulating behavior at 2.4 GPa.[37] Unlike the case of $P$-induced semiconducting state in $CeRu_4Sb_{12}$, the application of magnetic field to $PrFe_4P_{12}$ up to 4 T drastically suppressed the $P$-induced insulating state and recovered the heavy fermion behavior with an $A$ value comparable to that at zero field. Also in Kondo-semiconductor $CeOs_4Sb_{12}$, the semiconducting state was reported to be sensitive to magnetic field.[38] However, the mechanism of the $P$-induced metal-insulator (-semiconductor) transition and their field effect have not been clarified yet.

We performed high-pressure x-ray diffraction measurements up to $\sim$14 GPa of $CeRu_4Sb_{12}$ to confirm whether the $P$-induced semiconductivity was triggered by a structural phase transition or not and to elucidate the relationship between the lattice constant $a$ and the energy gap $\Delta$ in the semiconducting state as will be discussed later. Figure 5 depicts the relative unit-cell volume ($V/V_0$), where $V_0$ is the volume at zero pressure, as a function of $P$ of $CeRu_4Sb_{12}$ at room temperature. The inset shows $a$ versus $P$. Dashed curves are fitted based on the following Birch-Murnaghan equation of state[39]:
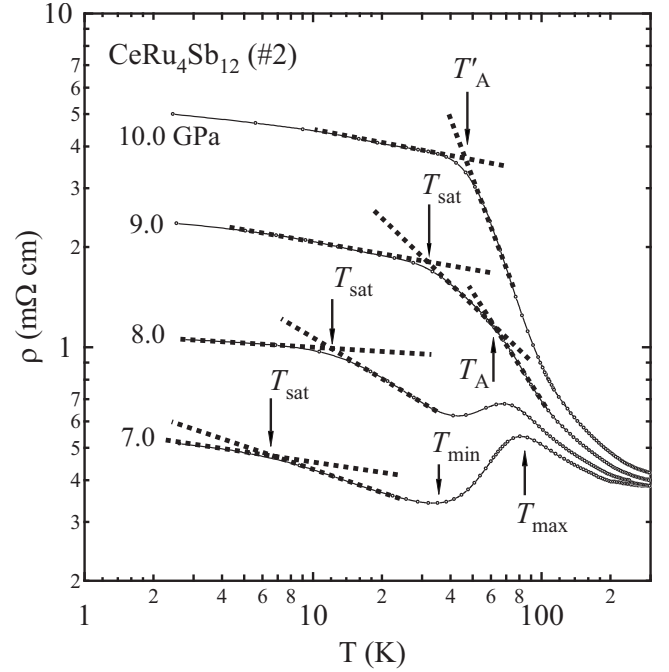


FIG. 6. Double-logarithmic plot of $\rho(T)$ at 7.0–10.0 GPa of $CeRu_4Sb_{12}$. $T_{sat}$, $T_A$, and $T'_A$ are determined as the temperature at which the two dashed lines drawn through the data points intersect. $T_A$ and $T'_A$ indicate the temperature where $T_{max}$ and $T_{min}$, and $T_A$ and $T_{sat}$ might come together, respectively.

$$P = \frac{3}{2}B_0\left\{\left(\frac{V}{V_0}\right)^{-7/3} - \left(\frac{V}{V_0}\right)^{-5/3}\right\}$$
$$\times\left[1 - \frac{3}{4}(4-B'_0)\left\{\left(\frac{V}{V_0}\right)^{-2/3} - 1\right\}\right]. \quad (1)$$

$V/V_0$ exhibits a monotonic decrease with increasing pressure without any indication of distinct structural change within the experimental error around 6.0 GPa where a $P$-induced metal-semiconductor transition showed up in $\rho(T)$. A fit of the data to the equation (1) yields a bulk modulus $B_0$ =89 GPa and its first pressure derivative $B'_0$=9.3. These numerical values obtained from a least-squares fit of the equation are comparable to a previous report and slightly smaller than that obtained by an ultrasonic experiment.[40,41] As seen in Ref. 40, $B_0$ in $CeRu_4Sb_{12}$ is comparable to that of $CeT_4Sb_{12}(T=Fe,Os)$ and is approximately half of that of $CeT_4P_{12}$ series.

## IV. DISCUSSION

### A. $T-P$ phase diagram

Figure 6 shows a double-logarithmic plot of $\rho(T)$ at 7.0–10.0 GPa of $CeRu_4Sb_{12}$. At $P \gtrsim 7.0$ GPa and LT region, $\rho(T)$ deviates from semiconducting behavior and tends to saturate toward a constant value. We define $T_{sat}$ where the saturation of resistivity has occurred as the temperature at which two dashed lines drawn through the data points intersect as shown in Fig. 6. With increasing pressure, $T_{sat}$ sharply shifts to HT as indicated by the arrows. At 9.0 and 10.0 GPa, broad
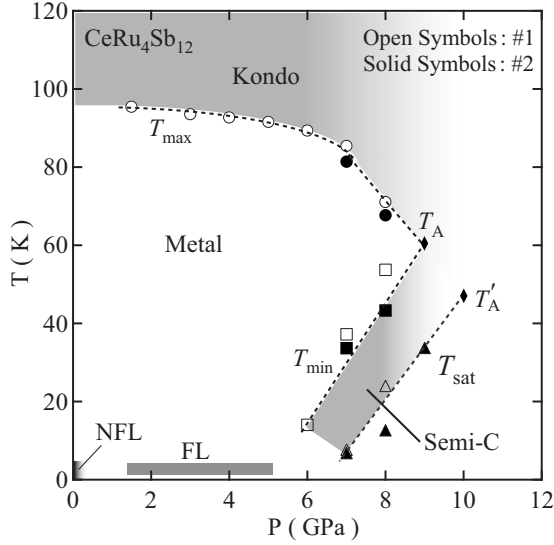
FIG. 7. A $T$−$P$ phase diagram of CeRu$_4$Sb$_{12}$. Open and closed symbols correspond to the data for samples 1 and 2, respectively. $T_{max}$, $T_{min}$, $T_{sat}$, and $T_A(T'_A)$ were signified by circles, squares, triangles, and diamonds, respectively. Semi-C, Kondo, FL, or NFL indicate the areas where electrical resistivity shows semiconducting, single-ion Kondo, FL, or NFL behavior, respectively. At 9.0 and 10.0 GPa, a boundary between semiconductor and Kondo is not clearly confirmed from the resistivity data.

peaks corresponding to $T_{max}$ and $T_{min}$ have disappeared. Instead, at 9.0 GPa, an anomalous behavior shows up as indicated by the change in slope denoted by $T_A$ in $\rho(T)$ around 60 K, possibly arising from nearly degenerate $T_{max}$ and $T_{min}$ temperature energy scales. Likewise, at 10.0 GPa, an anomaly in the resistivity marked as $T'_A$ may result from overlap of $T_A$ and $T_{sat}$. These indicate that the semiconducting behavior, which is confirmed between $T_{sat}$ and $T_{min}$ at 7.0 and 8.0 GPa, may overlap with single-ion Kondo one at 9.0 and 10.0 GPa around $T_A$ and $T'_A$, respectively. A deviation from semiconducting behavior in the resistivity is generally explainable by the existence of an impurity band. However, on account of the high quality samples employed in this study in which SdH and dHvA oscillations were clearly observed, the saturation of resistivity could originate from other intrinsic origins.[27,28] It should be noted that similar behavior has been observed in $\rho(T)$ of the Kondo-semiconductor CeOs$_4$Sb$_{12}$ under applied pressure below 5 K.[42] There is, up to now, no clear explanation about them. Similar $\rho(T)$ curves as observed at 9.0 and 10.0 GPa in CeRu$_4$Sb$_{12}$ have been reported for Kondo-insulator Ce$_3$Bi$_4$Pt$_3$ under high pressure.[43] The enhancement of resistivity at HT region became remarkable and shoulderlike behavior shifted to HT with increasing pressure in Ce$_3$Bi$_4$Pt$_3$. However, the upturn of resistivity at LT region was largely suppressed with pressure, contrary to the case of CeRu$_4$Sb$_{12}$. They suggested that there exist two different transport mechanisms of the gap formation in Ce$_3$Bi$_4$Pt$_3$: gap excitations at HT and gap-state transport at LT.

Figure 7 illustrates a temperature-pressure phase diagram of CeRu$_4$Sb$_{12}$. A semiconducting state which shows up at $P=6.0$ GPa below $T_{min}$ (semi-C) is shifted to higher tem-

perature with pressurization. On the other hand, single-ion Kondo effect above $T_{max}$ (Kondo) shifts to lower temperature as pressure increases. Due to overlapping of semiconductor with Kondo at 9.0 and 10.0 GPa, their boundary is not clearly confirmed from the resistivity data. In CeRu$_4$Sb$_{12}$, $T_{max}$ gradually shifts to lower temperature, drastically above 6.0 GPa, with increasing pressure. It is worth noting that the pressure variation of $T_{max}$ in CeRu$_4$Sb$_{12}$ is in strong contrast with that of typical Kondo-lattice Ce compounds such as CeCu$_6$ (Ref. 44) and CeAl$_3$ (Ref. 45) in which $T_{max}$ is proportional to $T_K$ and shifts to HT by applying pressure. In the case of CeRu$_4$Sb$_{12}$, $T_{max}$ could be caused by the competition between coherent behavior and semiconducting one, which may lead to the decrease of $T_{max}$ with applying pressure. Therefore, $T_K$ cannot be simply inferred from $T_{max}$ in resistivity in CeRu$_4$Sb$_{12}$.

### B. Energy gaps and lattice constants

The magnitude of the energy gap $\Delta$ in the semiconducting state of CeRu$_4$Sb$_{12}$ at $P \geq 6.0$ GPa is discussed. We presume the $P$-induced semiconducting state is described as a simple activated conduction law which obeys $\rho = C \exp(\Delta/T)$ where $C$ is constant. Figure 8 shows ln $\rho$ as a function of $1/T$ at several pressures: (a) 6.0–8.0 GPa (sample 1) and (b) 7.0–10.0 GPa (sample 2). The solid lines indicate the temperature where resistivity follows the activation law between $T_{sat}$ and $T_{min}(T_A)$, however in a narrow temperature regime. As shown in the inset of Fig. 8(a), fits to the activation yield small band gaps with the pressure derivative of the energy gap $d\Delta/dP=12.2$ and 11.5 K/GPa for samples 1 and 2, respectively. At 9.0 GPa, temperature range between $T_{sat}$ and $T_A$ is employed to estimate $\Delta$ since $T_A$ might be reminiscent of $T_{min}$ as mentioned above. At 9.0 GPa, unlike the data at $P=6.0$–8.0 GPa, distinct indication of semiconductivity is not observed and, hence, the magnitude of $\Delta$ varies depending on the temperature to be fitted. Two solid lines (around $T_{sat}$ or $T_{min}$) at 9.0 GPa in Fig. 8(b) correspond to the smallest or the largest value of $\Delta$, respectively. At 10.0 GPa, according to the merging of $T_A$ with $T_{min}$, $\Delta$ is not estimated in this paper. As for the temperature above $T_A$ at 9.0 GPa or $T'_A$ at 10.0 GPa, the upturn of resistivity is considered to be mainly due to single-ion Kondo scattering. It should be noted that, from resistivity data, the estimated $\Delta$ value is strongly influenced by LT coherent Kondo state or HT single-ion Kondo effect at low- or high-pressure region, respectively. The former suppresses the semiconducting behavior at low pressure of 6.0 GPa as seen in Fig. 2(a), which results in underestimation of $\Delta$. On the other hand, the merging of the semiconducting state with the latter could result in overestimation of $\Delta$ at high pressure of 9.0 or 10.0 GPa. In this regard, the $\Delta$ estimated at 7.0 or 8.0 GPa appears to be less affected by those effects.

By using the lattice constant $a$ and energy gap $\Delta$ of CeRu$_4$Sb$_{12}$ at each pressure obtained in this study (shown in Table I), we have determined the relationship between them for the purpose of comparing it to that of other Ce-based skutterudite compounds. Figure 9 shows the relationship between $\Delta$ and $a$ as a semilogarithmic plot of Ce$T_4X_{12}$ ($T$
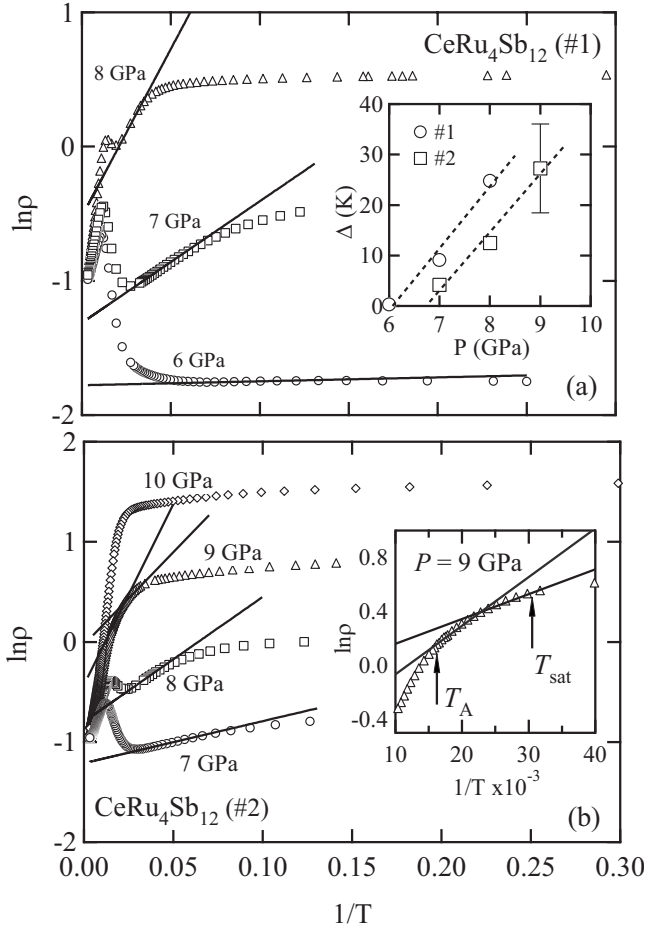
FIG. 8. $\rho$ versus $1/T$ of CeRu$_4$Sb$_{12}$ at several pressures: (a) 6.0–8.0 GPa (sample 1) and (b) 7.0–10.0 GPa (sample 2). Solid lines show the temperature where resistivity follows $\rho \propto \exp(\Delta/T)$ in the temperature range between $T_{sat}$ and $T_{min}$ ($T_A$). Inset in (a) shows the pressure dependence of $\Delta$ for samples 1 and 2. The edges of error bar at 9.0 GPa correspond to the value of $\Delta$ estimated in the temperature range just above $T_{sat}$ or just below $T_{min}$ as indicated by two solid lines in the inset of (b).
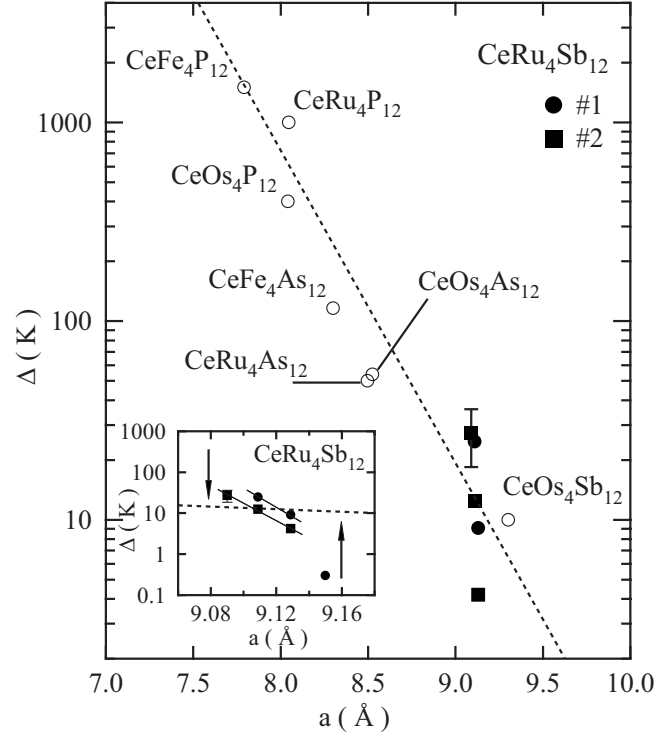


FIG. 9. Relationship between $\Delta$ and $a$ of the Ce-based skutterudite compounds which show semiconducting behavior and that of CeRu$_4$Sb$_{12}$ under high pressure as a semilogarithmic plot. Inset shows the expansion focusing on CeRu$_4$Sb$_{12}$. Dashed lines are drawn based on least-squares method.

$=$Fe, Ru, Os; $X=$P, As) including that of the $P$-induced semiconducting state in CeRu$_4$Sb$_{12}$.[5,15–18] As seen from a dashed line, log $\Delta$ almost linearly increases with decreasing $a$ in the CeT$_4$X$_{12}$ compounds. This fact indicates that the gap formation in these Ce compounds may be caused by the same $c$–$f$ hybridization manner, which is also inferred from the La-substitution results.[19,20] In the case of CeRu$_4$Sb$_{12}$, the trend that $\Delta$ increases with decreasing $a$ in CeRu$_4$Sb$_{12}$ is consistent with that of other Ce compounds. Note that, at

TABLE I. Comparison of $P$, $a$, and $\Delta$ which represent pressure, lattice constant, and energy gap estimated from activation law, respectively, in CeRu$_4$Sb$_{12}$.

| $P$ (GPa) | 6.0 | 7.0 | 8.0 | 9.0 | 10.0 |
|---|---|---|---|---|---|
| $a$ (Å) | 9.15 | 9.13 | 9.11 | 9.09 | 9.07 |
| $\Delta$ (K) (1) | 0.3 | 9.1 | 25 | | |
| $\Delta$ (K) (2) | | 4.2 | 12 | 12–29 | |

$P=8.0$ GPa ($a=9.1$ Å) where semiconducting behavior is relatively separated from LT coherent behavior or HT single-ion Kondo effect, $\Delta=12$ and 25 K for samples 1 and 2, respectively, are located near the dashed line between those of proximally positioned CeOs$_4$As$_{12}$ and CeOs$_4$Sb$_{12}$. However, magnitude of the slope for CeRu$_4$Sb$_{12}$ is remarkably greater than that of a dashed line even with consideration that the true slope for CeRu$_4$Sb$_{12}$ can be smaller as indicated by arrows because the obtained $\Delta$ value is underestimated or overestimated as mentioned. The reason why CeRu$_4$Sb$_{12}$ does not follow the dashed line has not been clarified yet. But it is considered that nature of the gap formation and the dependence of decreasing cell unit volume (or applying pressure) for $P$-induced semiconductivity in CeRu$_4$Sb$_{12}$ might be dominated by some as yet undetermined effects.

Finally, we consider how the metallic feature at ambient pressure changes into semiconducting one at LT by applying pressure (or decreasing lattice constant) in CeRu$_4$Sb$_{12}$. Application of external pressure enhances the $c$–$f$ hybridization and, in Ce compounds, widens the hybridization gap, which reduces the relative distance between the Fermi-level position and the top of the lower hybridization band. At large enough pressure above 5.0 GPa, it could lead to the transition from metallic to semiconducting at LT in CeRu$_4$Sb$_{12}$. Hence, the $P$-induced state in CeRu$_4$Sb$_{12}$ could be classified as a Kondo semiconductor which originates from the enhanced $c$–$f$ hybridization.

## V. SUMMARY

In summary, we have investigated the effect of high pressure on the electrical resistivity and structure of the filled skutterudite compound $CeRu_4Sb_{12}$. At $1.5 \leq P \leq 5.0$ GPa, $\rho(T)$ behavior is qualitatively the same as that at ambient pressure with the exception of a FL behavior at LT and an enhancement of humps of resistivity ascribed to single-ion Kondo scattering. At $P \geq 6.0$ GPa, $CeRu_4Sb_{12}$ exhibits a novel metal-semiconductor transition. The estimated $\Delta$ increases as pressure increases with a pressure coefficient of $d\Delta/dP \sim 12$ K/GPa. On the other hand, high-pressure x-ray diffraction of $CeRu_4Sb_{12}$ has revealed a monotonic decrease of $a$ up to $\sim 14.0$ GPa. The $P$-induced semiconducting behavior observed at $P \geq 6.0$ GPa in $CeRu_4Sb_{12}$ could be closely related to the enhanced $c-f$ hybridization by applying pressure and be classified as a Kondo semiconductor. In order to elucidate the $P$-induced semiconducting state, further experiments under high pressure are needed.

## ACKNOWLEDGMENTS

*Present address: Los Alamos National Laboratory, Los Alamos, New Mexico 87545, USA.

[1] G. P. Meisner, Physica B & C **108**, 763 (1981)

[2] L. E. DeLong and G. P. Meisner, Solid State Commun. **53**, 119 (1985).

[3] I. Shirotani, K. Ohno, C. Sekine, T. Yagi, T. Kawakami, T. Nakanishi, H. Takahashi, J. Tang, A. Matsushita, and T. Matsumoto, Physica B **281**, 1021 (2000).

[4] I. Shirotani, T. Uchiumi, K. Ohno, C. Sekine, Y. Nakazawa, K. Kanoda, S. Todo, and T. Yagi, Phys. Rev. B **56**, 7866 (1997).

[5] E. D. Bauer, A. Ślebarski, E. J. Freeman, C. Sirvent, and M. B. Maple, J. Phys.: Condens. Matter **13**, 4495 (2001).

[6] T. Uchiumi, I. Shirotani, C. Sekine, S. Todo, T. Yagi, Y. Nakazawa, and K. Kanoda, J. Phys. Chem. Solids **60**, 689 (1999).

[7] E. D. Bauer, N. A. Frederick, P.-C. Ho, V. S. Zapf, and M. B. Maple, Phys. Rev. B **65**, 100506(R) (2002).

[8] A. Kiss and Y. Kuramoto, J. Phys. Soc. Jpn. **75**, 103704 (2006).

[9] O. Sakai, J. Kikuchi, R. Shiina, H. Sato, H. Sugawara, M. Takigawa, and H. Shiba, J. Phys. Soc. Jpn. **76**, 024710 (2007).

[10] J. Kikuchi, M. Takigawa, H. Sugawara, and H. Sato, J. Phys. Soc. Jpn. **76**, 043705 (2007).

[11] N. Takeda and M. Ishikawa, J. Phys.: Condens. Matter **15**, L229 (2003).

[12] C. Sekine, T. Uchiumi, I. Shirotani, and T. Yagi, Phys. Rev. Lett. **79**, 3218 (1997).

[13] C. Sekine, H. Saito, T. Uchiumi, A. Sakai, and I. Shirotani, Solid State Commun. **106**, 441 (1998).

[14] K. Takegahara, H. Harima, and A. Yanase, J. Phys. Soc. Jpn. **70**, 1190 (2001).

[15] G. P. Meisner, M. S. Torikachvili, K. N. Yang, M. B. Maple, and R. P. Guertin, J. Appl. Phys. **57**, 3073 (1985).

[16] I. Shirotani, T. Uchiumi, C. Sekine, M. Hori, and S. Kimura, J. Solid State Chem. **142**, 146 (1999).

[17] F. Grandjean, A. Gerand, D. J. Braun, and W. Jeitschko, J. Phys. Chem. Solids **45**, 877 (1984).

[18] C. Sekine, N. Hoshia, K. Takeda, T. Yoshida, I. Shirotani, K. Matsuhira, M. Wakeshima, and Y. Hinatsu, Physica B (Amsterdam) **310**, 260 (2007).

[19] I. Shirotani, T. Uchiumi, C. Sekine, M. Hori, S. Kimura, and N. Hamaya, J. Solid State Chem. **142**, 146 (1999).

[20] H. Sugawara, S. Yuasa, A. Tsuchiya, Y. Aoki, H. Sato, T. Sasakawa, and T. Takabatake, Physica B **378-380**, 173 (2006).

[21] N. Takeda and M. Ishikawa, J. Phys. Soc. Jpn. **69**, 868 (2000).

[22] H. Harima (unpublished).

[23] S. V. Dordevic, D. N. Basov, N. R. Dilley, E. D. Bauer, and M. B. Maple, Phys. Rev. Lett. **86**, 684 (2001).

[24] D. T. Adroja, J.-G. Park, K. A. McEwen, N. Takeda, M. Ishikawa, and J.-Y. So, Phys. Rev. B **68**, 094425 (2003).

[25] T. Saso, J. Phys. Soc. Jpn. **75**, 043705 (2006).

[26] K. Abe, H. Sato, T. D. Matsuda, T. Namiki, H. Sugawara, and Y. Aoki, J. Phys.: Condens. Matter **14**, 11757 (2002).

[27] K. Abe, H. Sato, T. D. Matsuda, T. Namiki, H. Sugawara, and Y. Aoki, Physica B **312-313**, 256 (2002).

[28] H. Sugawara, K. Abe, T. D. Matsuda, Y. Aokia, H. Sato, R. Settai, and Y. Onuki, Physica B **312-313**, 264 (2002).

[29] E. D. Bauer, A. Ślebarski, R. P. Dickey, E. J. Freeman, C. Sirvent, V. S. Zapf, N. R. Dilley, and M. B. Maple, J. Phys.: Condens. Matter **13**, 5183 (2001).

[30] N. Takeda and M. Ishikawa, J. Phys.: Condens. Matter **13**, 5971 (2001).

[31] M. Kobayashi, S. R. Saha, H. Sugawara, T. Namiki, Y. Aoki, and H. Sato, Physica B **329-333**, 605 (2003).

[32] W. Jeitschko and D. J. Braun, Acta Crystallogr., Sect. B: Struct. Crystallogr. Cryst. Chem. **33**, 3401 (1977).

[33] F. Grandjean, A. Gérard, D. J. Braung, and W. Jeitschko, J. Phys. Chem. Solids **45**, 877 (1984).

[34] N. Kurita, M. Hedo, Y. Uwatoko, M. Kobayashi, H. Sugawara, H. Sato, and N. Môri, J. Magn. Magn. Mater. **272-276**, e81 (2004).

[35] N. Môri, H. Takahashi, and N. Takeshita, High Press. Res. **24**, 225 (2004).

[36] B. Cornut and B. Coqblin, Phys. Rev. B **5**, 4541 (1972).

[37] H. Hidaka, I. Ando, H. Kotegawa, T. C. Kobayashi, H. Harima, M. Kobayashi, H. Sugawara, and H. Sato, Phys. Rev. B **71**, 073102 (2005).

[38] H. Sugawara, S. Osaki, M. Kobayashi, T. Namiki, S. R. Saha, Y. Aoki, and H. Sato, Phys. Rev. B **71**, 125127 (2005).

[39] F. Birch, Phys. Rev. **71**, 809 (1947).

[40] I. Shirotani, T. Noro, J. Hayashi, C. Sekine, R. Giri, and T. Kikegawa, J. Phys.: Condens. Matter **16**, 7853 (2004).

[41] Y. Nakanishi, T. Yamaguchi, H. Hazawa, T. Goto, T. D. Matsuda, H. Sugawara, H. Sato, and M. Yoshizawa, J. Phys. Soc. Jpn. **70**, 249 (2002).

[42] M. Hedo, Y. Uwatoko, H. Sugawara, and H. Sato, Physica B **329-333**, 456 (2003).

[43] J. C. Cooley, M. C. Aronson, and P. C. Canfield, Phys. Rev. B **55**, 7533 (1997).

[44] A. Shibata, G. Oomi, Y. Ōnuki, and T. Komatsubara, J. Phys. Soc. Jpn. **55**, 2086 (1986).

[45] T. Kagayama and G. Oomi, J. Phys. Soc. Jpn. **65**, 42 (1996).